

¹ The human visual system preserves the hierarchy
² of 2-dimensional pattern regularity

³ Peter J. Kohler^{1,2,3} and Alasdair D. F. Clarke⁴

⁴ *¹ York University, Department of Psychology, Toronto, ON M3J 1P3, Canada*

⁵ *² Centre for Vision Research, York University, Toronto, ON, M3J 1P3, Canada*

⁶ *³Stanford University, Department of Psychology, Stanford, CA 94305, United States*

⁷ *⁴University of Essex, Department of Psychology, Colchester, UK, CO4 3SQ*

⁸ **Abstract**

Symmetries are present at many scales in images of natural scenes. A large body of literature has demonstrated contributions of symmetry to numerous domains of visual perception. The four fundamental symmetries, reflection, rotation, translation and glide reflection, can be combined in exactly 17 distinct ways. These *wallpaper groups* represent the complete set of symmetries in 2D images and have recently found use in the vision science community as an ideal stimulus set for studying the perception of symmetries in textures. The goal of the current study is to provide a more comprehensive description of responses to symmetry in the human visual system, by collecting both brain imaging (Steady-State Visual Evoked Potentials measured using high-density EEG) and behavioral (symmetry detection thresholds) data using the entire set of wallpaper groups. This allows us to probe the hierarchy of complexity among wallpaper groups, in which simpler groups are subgroups of more complex ones. We find that this hierarchy is preserved almost perfectly in both behavior and brain activity: A multi-level Bayesian GLM indicates that for most of the 63 subgroup relationships, subgroups produce lower amplitude responses in visual cortex (posterior probability: > 0.95 for 56 of 63) and require longer presentation durations to be reliably detected (posterior probability: > 0.95 for 49 of 63). This systematic pattern is seen only in visual cortex and only in components of the brain response known to be symmetric-specific. Our results show that representations of symmetries in the human brain are precise and rich in detail, and that this precision is reflected in behavior. These findings expand our understanding of symmetry perception, and open up new avenues for research on how fine-grained representations of regular textures contribute to natural vision.

Symmetries are abundant in natural and man-made environments, due to a complex interplay of physical forces that govern pattern formation in nature. Symmetrical patterns have been created and appreciated by human cultures throughout history and since the gestalt movement of the early 20th century, symmetry has been recognized as important for visual perception. Symmetry contributes to the perception of shapes (Palmer, 1985; Li et al., 2013), scenes (Apthorp and Bell, 2015) and surface properties (Cohen and Zaidi, 2013), as well as the social process of mate selection (Møller, 1992). Most of this work has focused on mirror symmetry or *reflection*, with much less attention being paid to the other fundamental symmetries: *rotation*, *translation*

and *glide reflection*. In the two spatial dimensions relevant for images, these four symmetries can be combined in 17 distinct ways, *the wallpaper groups* (Fedorov, 1891; Polya, 1924; Liu et al., 2010). Previous work on a subset of four of the wallpaper groups used functional MRI to demonstrate that rotation symmetries in wallpapers elicit parametric responses in several areas in occipital cortex, beginning with visual area V3 (Kohler et al., 2016). This effect was also robust with electroencephalography (EEG), whether measured using Steady-State Visual Evoked Potentials (SSVEPs) (Kohler et al., 2016) or event-related paradigms (Kohler et al., 2018). Here we extend this work by collecting SSVEPs and psychophysical data from human participants viewing the full set of wallpaper groups. We measure responses in visual cortex to 16 out of the 17 wallpaper groups, with the 17th serving as a control stimulus. Our goal is to provide a more complete picture of how wallpaper groups are represented in the human visual system.

A wallpaper group is a topologically discrete group of isometries of the Euclidean plane, i.e. transformations that preserve distance (Liu et al., 2010). The wallpaper groups differ in the number and kind of these transformations and we can uniquely refer to different groups using crystallographic notation. In brief, most groups are notated by PXZ , where $X \in \{1, 2, 3, 4, 6\}$ indicates the highest order of rotational symmetry and $Z \in \{m, g\}$ indicates whether the pattern contains mirror or glide symmetry. For example, $P4$ contains 4 fold rotation, while $P2M$ contains 2 fold rotation and a mirror symmetry (see Figure XXX). Two of the groups start with a C rather than a P , (CM and CMM) which indicates that the symmetries are specified relative to a cell that itself contains repetition. Full details of the naming convention and examples of the wallpaper groups can be found on wikipedia.

In mathematical group theory, when the elements of one group is completely contained in another, the inner group is called a subgroup of the outer group (Liu et al., 2010). The full list of subgroup relationships is listed in Section 1.4.2 of the Supplementary Material. Subgroup relationships between wallpaper groups can be distinguished by their indices. The index of a subgroup relationship is the number of cosets, i.e. the number of times the subgroup is found in the supergroup (Liu et al., 2010). As an example, let us consider groups P_2 and P_6 . If we ignore the translations in two directions that both groups share, group P_6 consists of the set of rotations $\{0^\circ, 60^\circ, 120^\circ, 180^\circ, 240^\circ, 300^\circ\}$, in which $P_2 \{0^\circ, 180^\circ\}$ is contained. P_2 is thus a subgroup of P_6 , and P_6 can be generated by combining P_2 with rotations $\{0^\circ, 120^\circ, 240^\circ\}$. Because P_2 is repeated three times in P_6 , P_2 is a subgroup of P_6 with index 3 (Liu et al., 2010). The 17 wallpaper groups thus obey a hierarchy of complexity where simpler groups are subgroups of more complex ones (Coxeter and Moser, 1972).

The two datasets we present here make it possible to assess the extent to which both behavior and brain responses follow the hierarchy of complexity expressed by the subgroup relationships. Based on previous brain imaging work showing that patterns with more axes of symmetry produce greater activity in visual cortex (Sasaki et al., 2005; Tyler et al., 2005; Kohler et al., 2018, 2016; Keefe et al., 2018), we hypothesized that more complex groups would produce larger SSVEPs. For the psychophysical data, we hypothesized that more complex groups would lead to shorter symmetry detection thresholds, based on previous data showing that under a fixed presentation time, discriminability increases with the number of symmetry axes in the pattern (Wagemans

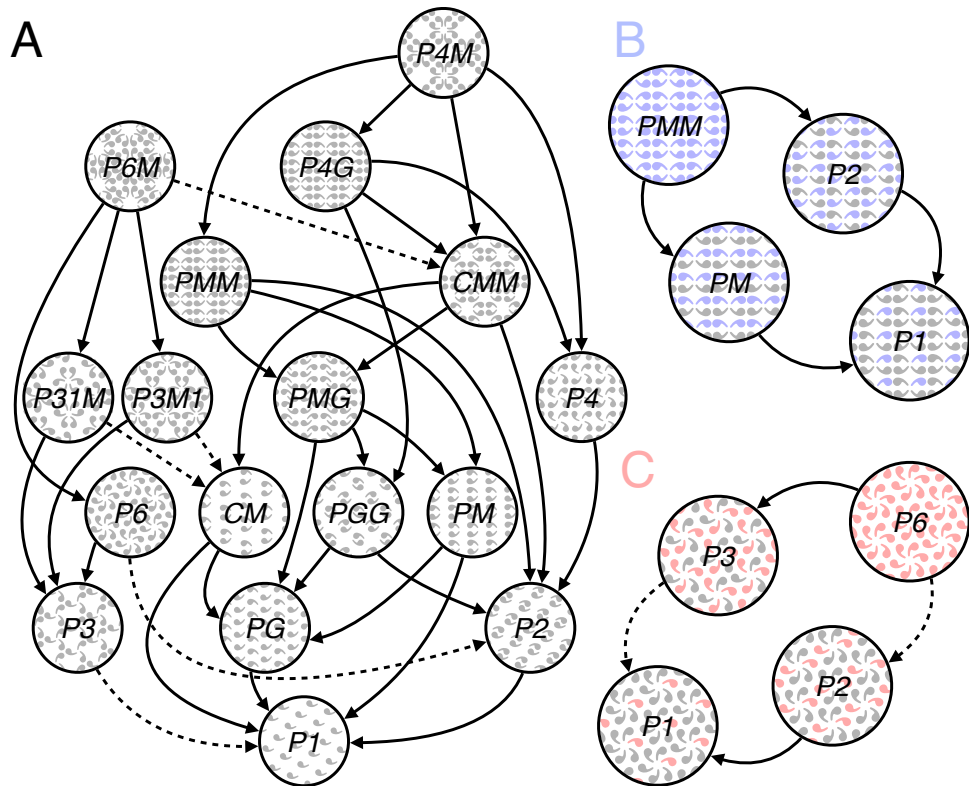


Figure 1: Subgroup relationships within indices 2 (solid lines) and 3 (dashed line) are shown in (A). All other relationships can be inferred by identifying the shortest path through the hierarchy, and multiplying the subgroup indices. For example, P_1 is related to P_6 through $P_6 \rightarrow P_3$ (index 2) and $P_3 \rightarrow P_1$ (index 3) so P_1 is also a subgroup of P_6 with index $3 \times 2 = 6$. We also show enlarged versions of some of the subgroup relationships involving PMM (B, shown in blue) and P_6 (C, shown in red) and highlight the symmetries within the subgroups to emphasize how the supergroup can be generated by adding additional transformations to the subgroup.

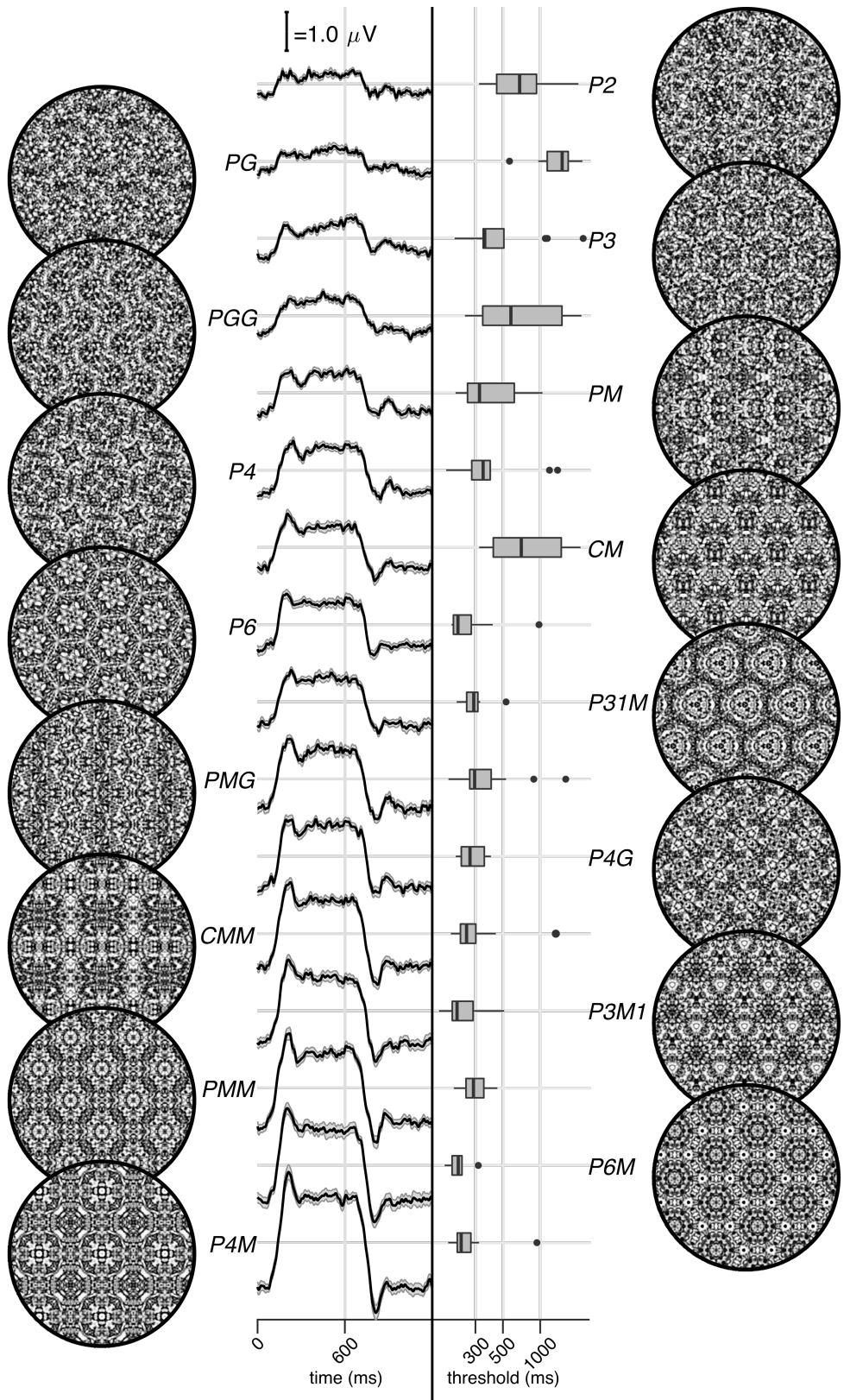


Figure 2: Examples of each of the 16 wallpaper groups are shown in the left- and right-most column of the figures, next to the corresponding SSVEP (center-left) and psychological (center-right) data from each group. The SSVEP data are odd-harmonic-filtered cycle-average waveforms. In each cycle, a P_1 exemplar was shown for the first 600 ms, followed by the original exemplar for the last 600 ms. Errorbars are standard error of the mean. Psychophysical data are presented as boxplots reflecting the distribution of display duration thresholds. The 16 groups are ordered by the strength of the SSVEP response, to highlight the range of response amplitudes.

79 et al., 1991). Our results confirm both hypotheses, and show that activity in human visual cortex
80 is remarkably consistent with the hierarchical relationships between the wallpaper groups, with
81 SSVEP amplitudes and psychophysical thresholds following these relationships at a level that is
82 far beyond chance. The human visual system thus appears to encode all of the fundamental sym-
83 metries using a representational structure that closely approximates the subgroup relationships
84 from group theory.

85 Results

86 The stimuli used in our two experiments were generated from random-noise textures, which
87 made it possible to generate multiple exemplars from each of the wallpaper groups, as described
88 in detail elsewhere (Kohler et al., 2016). We generated control stimuli matched to each exemplar
89 in the main stimulus set, by scrambling the phase but maintaining the power spectrum. All
90 wallpaper groups are inherently periodic because of their repeating lattice structure. Phase
91 scrambling maintains this periodicity, so the phase-scrambled control images all belong to group
92 P_1 regardless of group membership of the original exemplar. P_1 contains no symmetries other
93 than translation, while all other groups contain translation in combination with one or more of the
94 other three fundamental symmetries (reflection, rotation, glide reflection) (Liu et al., 2010). In our
95 SSVEP experiment, this stimulus set allowed us to isolate brain activity specific to the symmetry
96 structure in the exemplar images from activity associated with modulation of low-level features,
97 by alternating exemplar images and control exemplars. In this design, responses to structural
98 features beyond the shared power spectrum, including any symmetries other than translation,
99 are isolated in the odd harmonics of the image update frequency (Kohler et al., 2016; Norcia et al.,
100 2015, 2002). Thus, the combined magnitude of the odd harmonic response components can be
101 used as a measure of the overall strength of the visual cortex response.

102 The psychophysical experiment took a distinct but related approach. In each trial an exemplar
103 image was shown with its matched control, one image after the other, and the order varied pseudo-
104 randomly such that in half the trials the original exemplar was shown first, and in the other half
105 the control image was shown first. After each trial, participants were instructed to indicate
106 whether the first or second image contained more structure. The duration of both images was
107 controlled by a staircase procedure so that a threshold duration for symmetry detection could be
108 computed for each wallpaper group.

109 Examples of the wallpaper groups and a summary of our brain imaging and psychophysical
110 measurements are shown in Figure 2. For our primary SSVEP analysis, we only considered EEG
111 data from a pre-determined region-of-interest (ROI) consisting of six electrodes over occipital cor-
112 tex (see Supplementary Figure 1.1). SSVEP data from this ROI was filtered so that only the odd
113 harmonics that capture the symmetry response contribute to the waveforms. While waveform am-
114 plitude is quite variable among the 16 groups, all groups have a sustained negative-going response
115 that begins at about the same time for all groups, 180 ms after the transition from the P_1 control
116 exemplar to the original exemplar. To reduce the amplitude of the symmetry-specific response to
117 a single number that could be used in further analyses and compared to the psychophysical data,

we computed the root-mean-square (RMS) over the odd-harmonic-filtered waveforms. The data in Figure 2 are shown in descending order according to RMS. The psychophysical results, shown in box plots in Figure 2, were also quite variable between groups, and there seems to be a general pattern where wallpaper groups near the top of the figure, that have lower SSVEP amplitudes, also have longer psychophysical threshold durations.

We now wanted to test our two hypotheses about how SSVEP amplitudes and threshold durations would follow subgroup relationships, and thereby quantify the degree to which our two measurements were consistent with the group theoretical hierarchy of complexity. We tested each hypothesis using the same approach. We first fitted a Bayesian model with wallpaper group as a factor and participant as a random effect. We fit the model separately for SSVEP RMS and psychophysical data and then computed posterior distributions for the difference between supergroup and subgroup. These difference distributions allowed us to compute the conditional probability that the supergroup would produce (a) larger RMS and (b) a shorter threshold durations, when compared to the subgroup. The posterior distributions are shown in Figure 3 for the SSVEP data, and in Figure 4 for the psychophysical data, which distributions color-coded according to conditional probability. For both data sets our hypothesis is confirmed: For the overwhelming majority of the 63 subgroup relationships, supergroups are more likely to produce larger symmetry-specific SSVEPs and shorter symmetry detection threshold durations, and in most cases the conditional probability of this happening is extremely high.

We also ran a control analysis using (1) odd-harmonic SSVEP data from a six-electrode ROI over parietal cortex (see Supplementary Figure 1.1) and (2) even-harmonic SSVEP data from the same occipital ROI that was used in our primary analysis. By comparing these two control analysis to our primary SSVEP analysis, we can address the specify of our effects in terms of location (occipital cortex vs parietal cortex) and harmonic (odd vs even). For both control analyses (plotted in Supplementary Figures 3.3 and 3.4), the correspondence between data and subgroup relationships was substantially weaker than in the primary analysis. We can quantify the strength of the association between the data and the subgroup relationships, by asking what proportion of subgroup relationships that reach or exceed a range of probability thresholds. This is plotted in Figure 5, for our psychophysical data, our primary SSVEP analysis and our two control SSVEP analyses. It shows that odd-harmonic SSVEP data from the occipital ROI and symmetry detection threshold durations both have a strong association with the subgroup relationships such that a clear majority of the subgroups survive even at the highest threshold we consider ($p(\Delta > 0 | data) > 0.99$). The association is far weaker for the two control analyses.

SSVEP data from four of the wallpaper groups (P_2 , P_3 , P_4 and P_6) was previously published as part of our earlier demonstration of parametric responses to rotation symmetry in wallpaper groups (Kohler et al., 2016). We replicate that result using our Bayesian approach, and find an analogous parametric effect in the psychophysical data (see Supplementary Figure 4.1). We also conducted an analysis testing for an effect of index in our two datasets and found that subgroup relationships with higher indices tended to produce greater pairwise differences between the subgroup and supergroup, for both SSVEP RMS and symmetry detection thresholds (see Supplementary Figure 4.2). The effect of index is relatively weak, but the fact that there is a measurable

159 index effect can nonetheless be taken as preliminary evidence that representations of symmetries
160 in wallpaper groups may be compositional.

161 Finally, we conducted a correlation analysis comparing SSVEP and psychophysical data and
162 found a reliable correlation ($R^2 = 0.44$, Bayesian confidence interval [0.28, 0.55]). The correlation
163 reflects an inverse relationship: For subgroup relationships where the supergroup produces a
164 much *larger* SSVEP amplitude than the subgroup, the supergroup also tends to produce a much
165 *smaller* symmetry detection threshold. This is consistent with our hypotheses about how the
166 two measurements relate to symmetry representations in the brain, and suggests that our brain
167 imaging and psychophysical measurements are at least to some extent tapping into the same
168 underlying mechanisms.

169 Discussion

170 Here we show that beyond merely responding to the elementary symmetry operations of reflec-
171 tion (Sasaki et al., 2005; Tyler et al., 2005) and rotation (Kohler et al., 2016), the visual system
172 represents the hierarchical structure of the 17 wallpaper groups, and thus every composition of
173 the four fundamental symmetries (rotation, reflection, translation, glide reflection) which com-
174 prise the set of regular textures. Both SSVEP amplitudes and symmetry detection thresholds
175 preserve the hierarchy of complexity among the wallpaper groups that is captured by the sub-
176 group relationships (Coxeter and Moser, 1972). For the SSVEP, this remarkable consistency was
177 specific to the odd harmonics of the stimulus frequency that are known to capture the symmetry-
178 specific response (Kohler et al., 2016) and to electrodes in a region-of-interest (ROI) over occipital
179 cortex. When the same analysis was done using the odd harmonics from electrodes over parietal
180 cortex (Supplementary Figure 3.3) or even harmonics from electrodes over occipital cortex (Sup-
181 plementary Figure 3.4), the data was substantially less consistent with the subgroup relationships
182 (yellow and green lines, Figure 5).

183 The current data provide a description of the visual system's response to the complete set of
184 symmetries in the two-dimensional plane. Our design precludes us from independently measure
185 the response to P_1 , but because each of the 16 other groups produce non-zero odd harmonic
186 amplitudes (see Figure 2), we can conclude that the relationships between P_1 and all other groups,
187 where P_1 is the subgroup, are also preserved by the visual system. The subgroup relationships
188 are in many cases not obvious perceptually, and most participants had no knowledge of group
189 theory. Thus, the visual system's ability to preserve the subgroup hierarchy does not depend
190 on explicit knowledge of the relationships. Previous brain-imaging studies have found evidence
191 of parametric responses with the number of reflection symmetry folds Keefe et al. (2018); Sasaki
192 et al. (2005); Makin et al. (2016) and with the order of rotation symmetry Kohler et al. (2016).
193 Our study is the first demonstration that the brain encodes symmetry in this parametric fashion
194 across every possible combination of different *symmetry types*, and that this parametric encoding
195 is also reflected in behavior. Previous behavioral experiments have shown that although naïve
196 observers can distinguish many of the wallpaper groups (Landwehr, 2009), they tend to sort
197 them into fewer groups than there actually are (4-12 groups) and it is common for exemplars

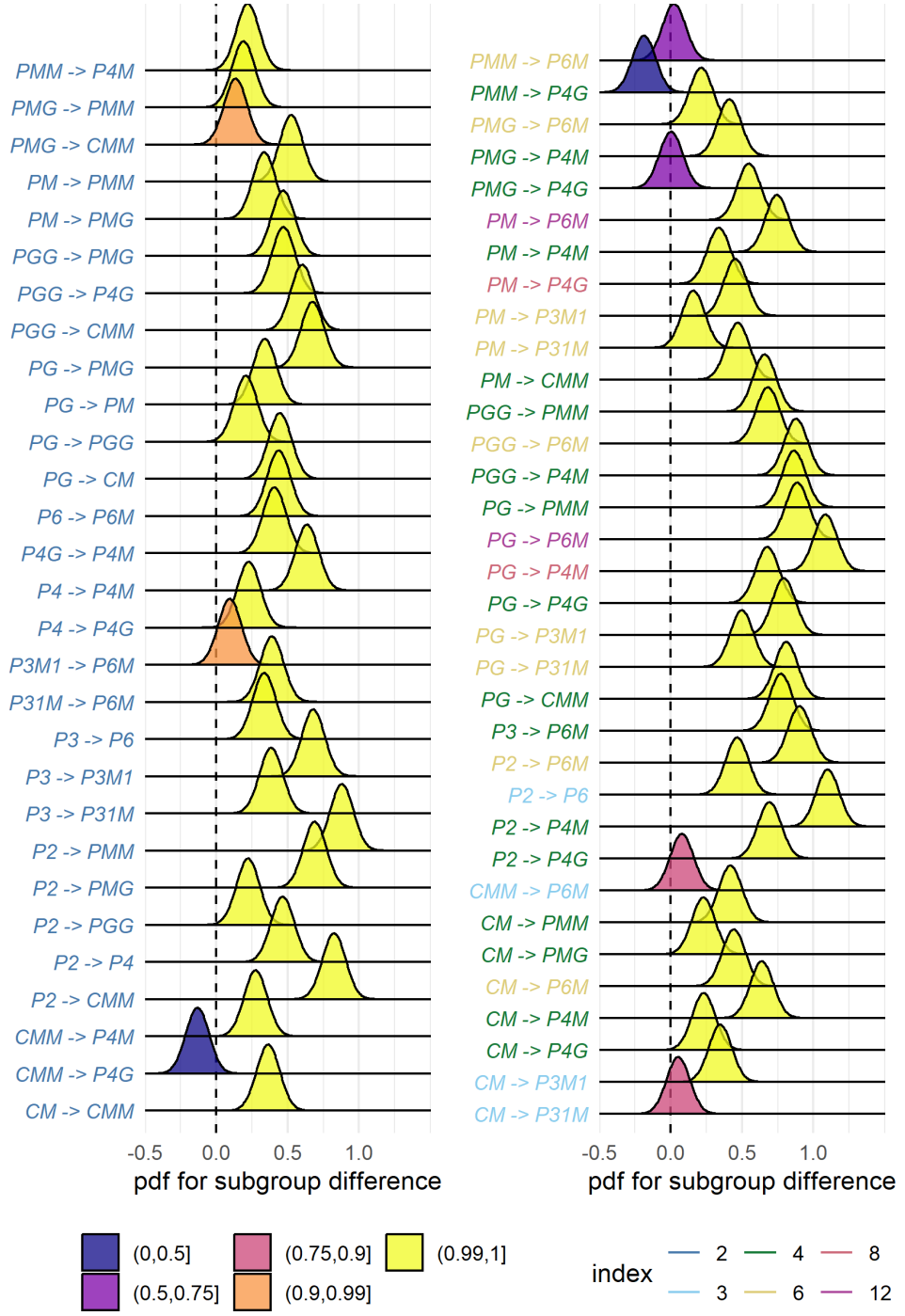


Figure 3: Posterior distributions for the difference in mean SSVEP RMS amplitude. Colour coding of the text indicates the index of the subgroup, while the colour of the filled distribution relates to the conditional probability that the difference in means is greater than zero. We can see that 55/63 subgroup relationships have $p(\Delta|data) > 0.99$.

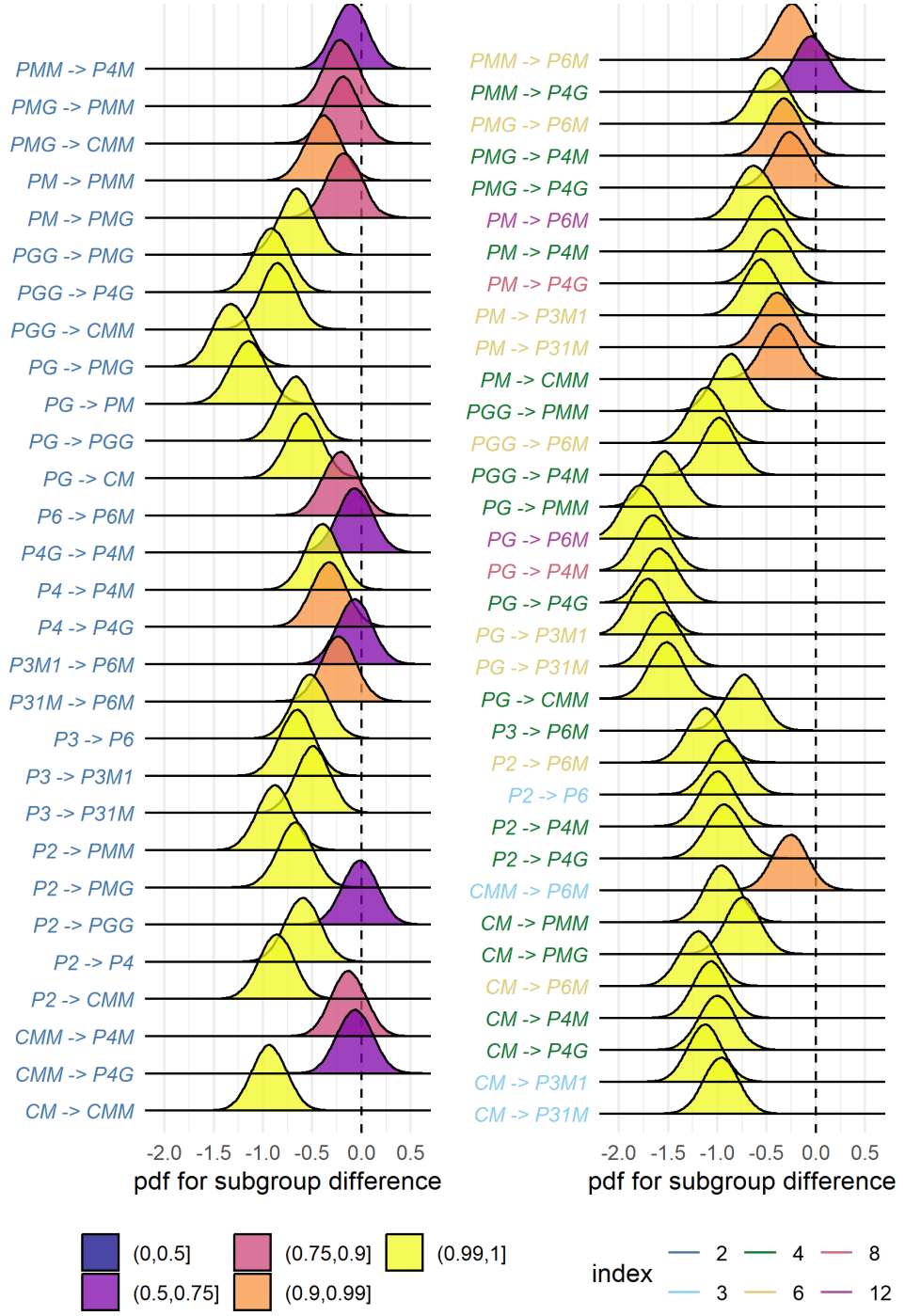


Figure 4: Posterior distributions for the difference in mean symmetry detection threshold durations. Colour coding of the text indicates the index of the subgroup, while the colour of the filled distribution relates to the conditional probability that the difference in means is greater than zero. We can see that 43/63 subgroup relationships have $p(\Delta|data) > 0.99$.

198 from different wallpaper groups to be sorted in the same group (Clarke et al., 2011). The more
199 controlled two-interval forced choice approach used in the current behavioral experiment allows
200 us to show that more granular representations of wallpaper groups are measurable in behavior.

201 A large literature exists on the *Sustained Posterior Negativity* (SPN), a characteristic negative-
202 going waveform that is known to reflect responses to symmetry and other forms of regularity
203 and structure (Makin et al., 2016). The SPN scales with the proportion of reflection symmetry
204 in displays that contain a mixture of symmetry and noise Makin et al. (2020); Palumbo et al.
205 (2015), and both reflection, rotation and translation can produce a measurable SPN Makin et al.
206 (2013). It has recently been demonstrated that a holographic model of regularity (van der Helm
207 and Leeuwenberg, 1996), can predict both SPN amplitude (Makin et al., 2016) and perceptual
208 discrimination performance (Nucci and Wagemans, 2007) for dot patterns that contain symmetry
209 and other types of regularity. The available evidence suggests that the SPN and our SSVEP
210 measurements are two distinct methods of isolating the same symmetry-related brain response:
211 When observed in the time-domain, the symmetry-selective odd-harmonic responses produce
212 similarly sustained waveforms (see Figure 2), odd-harmonic SSVEP responses can be measured
213 for dot patterns similar to those used to measure the SPN (Norcia et al., 2002), and the one event-
214 related study that has been published on the wallpaper groups also produced SPN-like waveforms
215 (Kohler et al., 2018). Future work should more firmly establish the connection and determine if
216 the SPN can capture responses similarly precise symmetry responses as the SSVEPs presented
217 here. It would also be worthwhile to ask if and how W can be computed for our random-noise based
218 wallpaper textures where combinations of symmetries tile the plane.

219 We observe a reliable correlation between our brain imaging and psychophysical data. This
220 suggests that the two measurements reflect the same underlying symmetry representations in
221 visual cortex. It should be noted that the correlation is relatively modest ($R^2 = 0.44$). This
222 may be partly due to the fact that different individuals participated in the two experiments.
223 It may also be related to the fact that participants were not doing a symmetry-related task
224 during the SSVEP experiment, but instead monitored the stimuli for brief, intermittent contrast
225 changes. Previous brain imaging studies have found enhanced reflection symmetry responses
226 when participants performed a symmetry-related task Makin et al. (2020); Sasaki et al. (2005); Keefe
227 et al. (2018). We did not manipulate task during our SSVEP recordings, but it is possible that
228 adding a symmetry-related task to our SSVEP experiment would have produced measurements
229 that reflected subgroup relationships to an even higher extent. We note, however, that our
230 performance is already close to ceiling (see Figure 5). It is possible that adding a symmetry-
231 related task would enhance SSVEP amplitudes across all wallpaper groups without improving
232 the discriminability of individual groups (similar to what was observed by Keefe and his co-authors
233 Keefe et al. (2018)). SPN measurements suggest that task-driven processing may be important
234 for detecting symmetries that have been subject to perspective distortion Makin et al. (2015)
235 although it should be noted that this effect was much less clear in a subsequent functional MRI
236 study Keefe et al. (2018). Future work in which behavioral and brain imaging data are collected
237 from the same participants, and behavior is manipulated in the SSVEP task, will help further
238 establish the connection between the two measurements, and elucidate the potential contribution

239 of task-related top-down processing to the current results.

240 We also find an effect of index for both our brain imaging measurements and our symmetry
241 detection thresholds. This means that the visual system not only represents the hierarchical rela-
242 tionship captured by individual subgroups, but also distinguishes between subgroups depending
243 on how many times the subgroup is repeated in the supergroup, with more repetitions leading
244 to larger pairwise differences. Our measured effect of index is relatively weak. This is perhaps
245 because the index analysis does not take into account the *type* of isometries that differentiate the
246 subgroup and supergroup. The effect of symmetry type can be observed by contrasting the mea-
247 sured SSVEP amplitudes and detection thresholds for groups *PM* and *PG* in Figure 2. The two
248 groups are comparable except *PM* contains reflection and *PG* contains glide reflection, and the
249 former clearly elicits higher amplitudes and lower thresholds. An important goal for future work
250 will be to map out how different symmetry types contribute to the representational hierarchy.

251 The correspondence between responses in the visual system and group theory that we demon-
252 strate here, may reflect a form of implicit learning that depends on the structure of the natural
253 world. The environment is itself constrained by physical forces underlying pattern formation
254 and these forces are subject to multiple symmetry constraints (Hoyle, 2006). The ordered struc-
255 ture of responses to wallpaper groups could be driven by a central tenet of neural coding, that of
256 efficiency. If coding is to be efficient, neural resources should be distributed to capture the struc-
257 ture of the environment with minimum redundancy considering the visual geometric optics, the
258 capabilities of the subsequent neural coding stages and the behavioral goals of the organism (At-
259 tneave, 1954; Barlow, 1961; Laughlin, 1981; Geisler et al., 2009). Early work within the efficient
260 coding framework suggested that natural images had a $1/f$ spectrum and that the corresponding
261 redundancy between pixels in natural images could be coded efficiently with a sparse set of ori-
262 ented filter responses, such as those present in the early visual pathway (Field, 1987; Olshausen
263 and Field, 1997). Our results suggest that the principle of efficient coding extends to a much
264 higher level of structural redundancy – that of symmetries in visual images.

265 The 17 wallpaper groups are completely regular, and relatively rare in the visual environment,
266 especially when considering distortions due to perspective (see above) and occlusion. Near-regular
267 textures, however, abound in the visual world, and can be modeled as deformed versions of the
268 wallpaper groups (Liu et al., 2004). The correspondence between visual cortex responses and
269 group theory demonstrated here may indicate that the visual system represents visual textures
270 using a similar scheme, with the wallpaper groups serving as anchor points in representational
271 space. This framework resembles norm-based encoding strategies that have been proposed for
272 other stimulus classes, most notably faces (Leopold et al., 2006), and leads to the prediction that
273 adaptation to wallpaper patterns should distort perception of near-regular textures, similar to
274 the aftereffects found for faces (Webster and MacLin, 1999). Field biologists have demonstrated
275 that animals respond more strongly to exaggerated versions of a learned stimulus, referred to
276 as “supernormal” stimuli (Tinbergen, 1953). In the norm-based encoding framework, wallpaper
277 groups can be considered *supertextures*, exaggerated examples of the near-regular textures that
278 surround us. Artists may consciously or unconsciously create supernormal stimuli, to capture the
279 essence of the subject and evoke strong responses in the audience (Ramachandran and Hirstein,

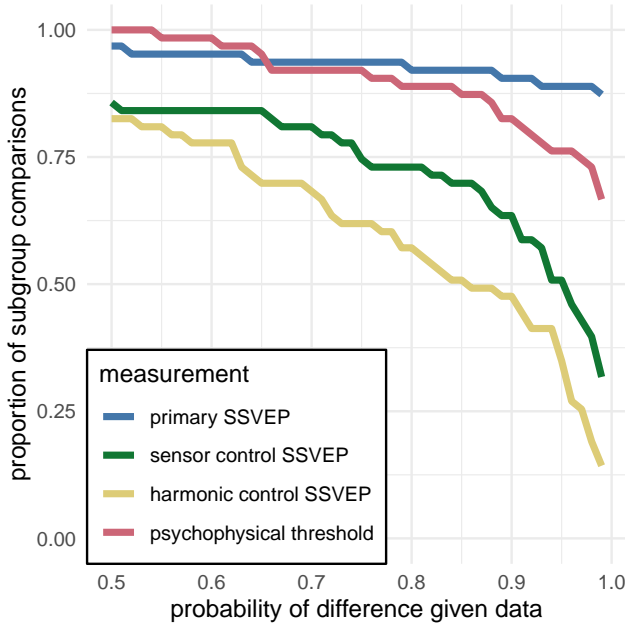


Figure 5: This plot shows the proportion of subgroup relationships that satisfy $p(\Delta > 0 | data) > x$. We can see that if we take $x = 0.95$ as our threshold, the subgroup relationships are preserved in $56/63 = 89\%$ and $48/63 = 76\%$ of the comparisons for the primary SSVEP and threshold duration datasets, respectively. This compares to the $32/63 = 51\%$ and $22/63 = 35\%$ for the SSVEP control datasets.

1999). Wallpaper groups are visually compelling, and symmetries have been widely used in
280 human artistic expression going back to the Neolithic age (Jablan, 2014). If wallpapers are in fact
281 supertextures, this prevalence may be a direct result of the strategy the human visual system has
282 adopted for texture encoding.
283

284 Participants

285 Twenty-five participants (11 females, mean age 28.7 ± 3.3) took part in the EEG experiment.
286 Their informed consent was obtained before the experiment under a protocol that was approved
287 by the Institutional Review Board of Stanford University. 11 participants (8 females, mean age
288 20.73 ± 1.21) took part in the psychophysics experiment. All participants had normal or corrected-to-normal vision. Their informed consent was obtained before the experiment under a protocol
289 that was approved by the University of Essex's Ethics Committee.
290

291 Stimulus Generation

292 Exemplars from the different wallpaper groups were generated using a modified version of the
293 methodology developed by Clarke and colleagues (Clarke et al., 2011) that we have described in de-
294 tail elsewhere (Kohler et al., 2016). Briefly, exemplar patterns for each group were generated from
295 random-noise textures, which were then repeated and transformed to cover the plane, according
296 to the symmetry axes and geometric lattice specific to each group. The use of noise textures as
297 the starting point for stimulus generation allowed the creation of an almost infinite number of

298 distinct exemplars of each wallpaper group. To make individual exemplars as similar as possible
299 we replaced the power spectrum of each exemplar with the median across exemplars within a
300 group. We then generated control exemplars that had the same power spectrum as the exemplar
301 images by randomizing the phase of each exemplar image. The phase scrambling eliminates ro-
302 tation, reflection and glide-reflection symmetries within each exemplar, but the phase-scrambled
303 images inherit the spectral periodicity arising from the periodic tiling. This means that all
304 control exemplars, regardless of which wallpaper group they are derived from, are transformed
305 into another symmetry group, namely P_1 . P_1 is the simplest of the wallpaper groups and contains
306 only translations of a region whose shape derives from the lattice. Because the different wallpaper
307 groups have different lattices, P_1 controls matched to different groups have different power spectra.
308 Our experimental design takes these differences into account by comparing the neural responses
309 evoked by each wallpaper group to responses evoked by the matched control exemplars.

310 Stimulus Presentation

311 Stimulus Presentation. For the EEG experiment, the stimuli were shown on a 24.5" Sony Trimas-
312 ter EL PVM-2541 organic light emitting diode (OLED) display at a screen resolution of 1920×1080
313 pixels, 8-bit color depth and a refresh rate of 60 Hz, viewed at a distance of 70 cm. The mean
314 luminance was 69.93 cd/m^2 and contrast was 95%. The diameter of the circular aperture in
315 which the wallpaper pattern appeared was 13.8° of visual angle presented against a mean lumi-
316 nance gray background. Stimulus presentation was controlled using in-house software. For the
317 psychophysics experiment, the stimuli were shown on a $48 \times 27\text{cm}$ VIEWPixed/3D LCD Display
318 monitor, model VPX-VPX-2005C, resolution 1920×1080 pixels, with a viewing distance of ap-
319 proximately 40cm and linear gamma. Stimulus presentation was controlled using MatLab and
320 Psychtoolbox-3 (Kleiner et al., 2007; Brainard, 1997). The diameter of the circular aperture for
321 the stimuli was 21.5° .

322 EEG Procedure

323 Visual Evoked Potentials were measured using a steady-state design, in which P_1 control images
324 alternated with exemplar images from each of the 16 other wallpaper groups. Exemplar images
325 were always preceded by their matched P_1 control image. A single 0.83 Hz stimulus cycle consisted
326 of a control P_1 image followed by an exemplar image, each shown for 600 ms. A trial consisted
327 of 10 such cycles (12 sec) over which 10 different exemplar images and matched controls from
328 the same rotation group were presented. For each group type, the individual exemplar images
329 were always shown in the same order within the trials. Participants initiated each trial with a
330 button-press, which allowed them to take breaks between trials. Trials from a single wallpaper
331 group were presented in blocks of four repetitions, which were themselves repeated twice per
332 session, and shown in random order within each session. To control fixation, the participants
333 were instructed to fixate a small white cross in the center of display. To control vigilance, a
334 contrast dimming task was employed. Two times per trial, an image pair was shown at reduced
335 contrast, and the participants were instructed to press a button on a response pad. We adjusted
336 the contrast reduction such that average accuracy for each participant was kept at 85% correct,

337 in order to keep the difficulty of the vigilance at a constant level.

338 Psychophysics Procedure

339 The experiment consisted of 16 blocks, one for each of the wallpaper groups (excluding P_1). We
340 used a two-interval forced choice approach. In each trial, participants were presented with two
341 stimuli (one of which was the wallpaper group for the current block of trials, the other being P_1),
342 one after the other (inter-stimulus interval of 700ms). After each stimulus had been presented, it
343 was masked with white noise for 300ms. After both stimuli had been presented, participants made
344 a response on the keyboard to indicate whether they thought the first or second image contained
345 more symmetry. Each block started with 10 practice trials, (stimulus display duration of 500ms)
346 to allow participants to familiarise themselves with the current block's wallpaper pattern. If they
347 achieved an accuracy of 9/10 in these trials they progressed to the rest of the block, otherwise
348 they carried out another set of 10 practise trials. This process was repeated until the required
349 accuracy of 9/10 was obtained. The rest of the block consisted of four interleaved staircases (using
350 the QUEST algorithm (Watson and Pelli, 1983), full details given in the SI) of 30 trials each. On
351 average, a block of trials took around 10 minutes to complete.

352 EEG Acquisition and Preprocessing

353 Steady-State Visual Evoked Potentials (SSVEPs) were collected with 128-sensor HydroCell Sensor
354 Nets (Electrical Geodesics, Eugene, OR) and were band-pass filtered from 0.3 to 50 Hz. Raw data
355 were evaluated off line according to a sample-by-sample thresholding procedure to remove noisy
356 sensors that were replaced by the average of the six nearest spatial neighbors. On average, less
357 than 5% of the electrodes were substituted; these electrodes were mainly located near the forehead
358 or the ears. The substitutions can be expected to have a negligible impact on our results, as the
359 majority of our signal can be expected to come from electrodes over occipital, temporal and parietal
360 cortices. After this operation, the waveforms were re-referenced to the common average of all
361 the sensors. The data from each 12s trial were segmented into five 2.4 s long epochs (i.e., each of
362 these epochs was exactly 2 cycles of image modulation). Epochs for which a large percentage of
363 data samples exceeding a noise threshold (depending on the participant and ranging between 25
364 and 50 μ V) were excluded from the analysis on a sensor-by-sensor basis. This was typically the
365 case for epochs containing artifacts, such as blinks or eye movements. Steady-state stimulation
366 will drive cortical responses at specific frequencies directly tied to the stimulus frequency. It is
367 thus appropriate to quantify these responses in terms of both phase and amplitude. Therefore, a
368 Fourier analysis was applied on every remaining epoch using a discrete Fourier transform with a
369 rectangular window. The use of two-cycle long epochs (i.e., 2.4 s) was motivated by the need to
370 have a relatively high resolution in the frequency domain, $\delta f = 0.42$ Hz. For each frequency bin,
371 the complex-valued Fourier coefficients were then averaged across all epochs within each trial.
372 Each participant did two sessions of 8 trials per condition, which resulted in a total of 16 trials
373 per condition.

374 **SSVEP Analysis**

375 Response waveforms were generated for each group by selective filtering in the frequency do-
376 main. For each participant, the average Fourier coefficients from the two sessions were averaged
377 over trials and sessions. The SSVEP paradigm we used allowed us to separate symmetry-related
378 responses from non-specific contrast transient responses. Previous work has demonstrated that
379 symmetry-related responses are predominantly found in the odd harmonics of the stimulus fre-
380 quency, whereas the even harmonics consist mainly of responses unrelated to symmetry, that
381 arise from the contrast change associated with the appearance of the second image (Norcia et al.,
382 2002; Kohler et al., 2016). This functional distinction of the harmonics allowed us to generate
383 a single-cycle waveform containing the response specific to symmetry, by filtering out the even
384 harmonics in the spectral domain, and then back-transforming the remaining signal, consisting
385 only of odd harmonics, into the time-domain. For our main analysis, we averaged the odd har-
386 monic single-cycle waveforms within a six-electrode region of interest (ROI) over occipital cortex
387 (electrodes 70, 74, 75, 81, 82, 83). These waveforms, averaged over participants, are shown in
388 Figure 2. The same analysis was done for the even harmonics and for the odd harmonics within a
389 six electrode ROI over parietal cortex (electrodes 53, 54, 61, 78, 79, 86; see Supplementary Figure
390 1.1). The root-mean square values of these waveforms, for each individual participant, were used
391 to determine whether each of the wallpaper subgroup relationships were preserved in the brain
392 data.

393 **Defining the list of subgroup relationships**

394 In order to get the complete list of subgroup relationships, we digitized Table 4 from Coxeter
395 (Coxeter and Moser, 1972) (shown in Supplementary Table 1.2). After removing identity rela-
396 tionships (i.e. each group is a subgroup of itself) and the three pairs of wallpaper groups that are
397 subgroups of each other (e.g. *PM* is a subgroup of *CM*, and *CM* is a subgroup of *PM*) we were left
398 with a total of 63 unambiguous subgroups that were included in our analysis.

399 **Bayesian Analysis of SSVEP and Psychophysical data**

400 Bayesian analysis was carried out using R (v3.6.1) (R Core Team, 2019) with the **brms** package
401 (v2.9.0) (Bürkner, 2017) and rStan (v2.19.2 (Stan Development Team, 2019)). The data from each
402 experiment were modelled using a Bayesian generalised mixed effect model with wallpaper group
403 being treated as a 16-level factor, and random effects for participant. The SSVEP data and sym-
404 metry detection threshold durations were modelled using log-normal distributions with weakly
405 informative, $\mathcal{N}(0, 2)$, priors. After fitting the model to the data, samples were drawn from the
406 posterior distribution of the two datasets, for each wallpaper group. These samples were then
407 recombined to calculate the distribution of differences for each of the 63 pairs of subgroup and
408 supergroup. These distributions were then summarised by computing the conditional probabil-
409 ity of obtaining a positive (negative) difference, $p(\Delta|\text{data})$. For further technical details, please
410 see the Supplementary Materials where the full R code, model specification, prior and posterior
411 predictive checks, and model diagnostics, can be found.

412 References

- 413 Apthorp, D. and Bell, J. (2015). Symmetry is less than
414 meets the eye. *Current Biology*, 25(7):R267–R268.
415 Attneave, F. (1954). Some informational aspects of
416 visual perception. *Psychol Rev*, 61(3):183–93.
417 Barlow, H. B. (1961). *Possible principles underlying the*
418 *transformations of sensory messages*, pages 217–234.
419 MIT Press.
420 Brainard, D. H. (1997). Spatial vision. *The psychophysics*
421 *toolbox*, 10:433–436.
422 Bürkner, P.-C. (2017). Advanced bayesian multilevel
423 modeling with the r package brms. *arXiv preprint*
424 *arXiv:1705.11123*.
425 Clarke, A. D. F., Green, P. R., Halley, F., and
426 Chantler, M. J. (2011). Similar symmetries: The
427 role of wallpaper groups in perceptual texture simi-
428 larity. *Symmetry*, 3(4):246–264.
429 Cohen, E. H. and Zaidi, Q. (2013). Symmetry in con-
430 text: Salience of mirror symmetry in natural pat-
431 terns. *Journal of vision*, 13(6).
432 Coxeter, H. S. M. and Moser, W. O. J. (1972). *Gen-
433 erators and relations for discrete groups*. *Ergebnisse*
434 *der Mathematik und ihrer Grenzgebiete*; Bd. 145
435 Springer-Verlag, Berlin, New York.
436 Fedorov, E. (1891). Symmetry in the plane. In *Za-
437 piski Imperatorskogo S. Peterburgskogo Mineralogicheskogo
438 Obshchestva [Proc. S. Peterb. Mineral. Soc.]*, volume 429
439 pages 345–390.
440 Field, D. J. (1987). Relations between the statistics
441 of natural images and the response properties of
442 cortical cells. *J Opt Soc Am A*, 4(12):2379–94.
443 Geisler, W. S., Najemnik, J., and Ing, A. D. (2009). Op-
444 timal stimulus encoders for natural tasks. *Journal*
445 *of Vision*, 9(13):17–17.
446 Hoyle, R. B. (2006). *Pattern formation: an introduction*
447 *to methods*. Cambridge University Press.
448 Jablan, S. V. (2014). *Symmetry, Ornament and Modular-
449 ity*. World Scientific Publishing Co Pte Ltd, Singapore,
450 SINGAPORE.
451 Keefe, B. D., Gouws, A. D., Sheldon, A. A., Vernon,
452 R. J. W., Lawrence, S. J. D., McKeefry, D. J., Wade,
453 A. R., and Morland, A. B. (2018). Emergence of
454 symmetry selectivity in the visual areas of the
455 human brain: fMRI responses to symmetry pre-
456 sented in both frontoparallel and slanted planes.
457 *Human Brain Mapping*, 39(10):3813–3826.
458 Kleiner, M., Brainard, D., Pelli, D., Ingling, A., Mur-
459 ray, R., and Broussard, C. (2007). What's new in
460 psychtoolbox-3. *Perception*, 36:1–16.
461 Kohler, P. J., Clarke, A., Yakovleva, A., Liu, Y., and
462 Norcia, A. M. (2016). Representation of maximally
463 regular textures in human visual cortex. *The Journal*
464 *of Neuroscience*, 36(3):714–729.
465 Kohler, P. J., Cottreau, B. R., and Norcia, A. M.
466 (2018). Dynamics of perceptual decisions about
467 symmetry in visual cortex. *NeuroImage*, 167(Sup-
468 pliment C):316–330.
469 Landwehr, K. (2009). Camouflaged symmetry. *Per-
470 ception*, 38:1712–1720.
471 Laughlin, S. (1981). A simple coding procedure en-
472 hances a neuron's information capacity. *Z Natur-
473 forsch C*, 36(9–10):910–2.
474 Leopold, D. A., Bondar, I. V., and Giese, M. A.
475 (2006). Norm-based face encoding by single neu-
476 rons in the monkey inferotemporal cortex. *Nature*,
477 442(7102):572–5.
478 Li, Y., Sawada, T., Shi, Y., Steinman, R., and Pizlo, Z.
479 (2013). *Symmetry Is the sine qua non of Shape*, book sec-
480 tion 2, pages 21–40. Advances in Computer Vision
481 and Pattern Recognition. Springer London.
482 Liu, Y., Hel-Or, H., Kaplan, C. S., and Van Gool,
483 L. (2010). Computational symmetry in computer
484 vision and computer graphics. *Foundations and
485 Trends® in Computer Graphics and Vision*, 5(1–2):1–
486 195.
487 Liu, Y., Lin, W.-C., and Hays, J. (2004). Near-regular
488 texture analysis and manipulation. In *ACM Trans-
489 actions on Graphics (TOG)*, volume 23, pages 368–
490 376. ACM.
491 Makin, A. D. J., Rampone, G., and Bertamini,
492 M. (2015). Conditions for view invariance

- 493 in the neural response to visual symmetry. *Psychophysiology*, 52(4):532–543. eprint 506
<https://onlinelibrary.wiley.com/doi/pdf/10.1111/psyp.12782>.
- 496 Makin, A. D. J., Rampone, G., Morris, A., and 503 Bertamini, M. (2020). The Formation of Symmetrical Gestalts Is Task-Independent, but Can Be Enhanced by Active Regularity Discrimination. *Journal of Cognitive Neuroscience*, 32(2):353–366. 510
 500 541
 501 Makin, A. D. J., Rampone, G., Pecchinenda, 508 A., and Bertamini, M. (2013). Electrophysiological responses to visuospatial regularity. 515 *Psychophysiology*, 50(10):1045–1055. eprint 514
<https://onlinelibrary.wiley.com/doi/pdf/10.1111/psyp.12082>.
 505 542
 506 Makin, A. D. J., Wright, D., Rampone, G., Palumbo, 513 L., Guest, M., Sheehan, R., Cleaver, H., and 548 Bertamini, M. (2016). An Electrophysiological Index of Perceptual Goodness. *Cerebral Cortex*, 26(12):4416–4434. 551
 507 547
 508
 509
 510
 511 Møller, A. P. (1992). Female swallow preference 512 for symmetrical male sexual ornaments. *Nature*, 357(6375):238–240. 554
 513
 514 Norcia, A. M., Appelbaum, L. G., Ales, J. M., Cottereau, B. R., and Rossion, B. (2015). The steady-state visual evoked potential in vision research: A review. *Journal of Vision*, 15(6):4–4. 558
 515 555
 516
 517
 518 Norcia, A. M., Candy, T. R., Pettet, M. W., Vildavski, V. Y., and Tyler, C. W. (2002). Temporal dynamics of the human response to symmetry. *Journal of Vision*, 2(2):132–139. 562
 519 559
 520
 521
 522 Nucci, M. and Wagemans, J. (2007). Goodness of Regularity in Dot Patterns: Global Symmetry, Local Symmetry, and Their Interactions. *Perception*, 36(9):1305–1319. Publisher: SAGE Publications Ltd STM. 566
 523 564
 524
 525
 526
 527 Olshausen, B. A. and Field, D. J. (1997). Sparse coding with an overcomplete basis set: a strategy employed by v1? *Vision Res*, 37(23):3311–25. 570
 528 569
 529
 530 Palmer, S. E. (1985). The role of symmetry in shape perception. *Acta Psychologica*, 59(1):67–90. 572
 531
 532 Palumbo, L., Bertamini, M., and Makin, A. (2015). Scaling of the extrastriate neural response to symmetry. *Vision Research*, 117:1–8. 575
 533 574
 534 Polya, G. (1924). Xii. Über die analogie der kristallsymmetrie in der ebene. *Zeitschrift für Kristallographie-Crystalline Materials*, 60(1):278–282.
- R Core Team (2019). *R: A Language and Environment for Statistical Computing*. R Foundation for Statistical Computing, Vienna, Austria.
- Ramachandran, V. S. and Hirstein, W. (1999). The science of art: A neurological theory of aesthetic experience. *Journal of Consciousness Studies*, 6(6–7):15–41.
- Sasaki, Y., Vanduffel, W., Knutson, T., Tyler, C., and Tootell, R. (2005). Symmetry activates extrastriate visual cortex in human and nonhuman primates. *Proceedings of the National Academy of Sciences of the United States of America*, 102(8):3159–3163.
- Stan Development Team (2019). RStan: the R interface to Stan. R package version 2.19.2.
- Tinbergen, N. (1953). *The herring gull's world: a study of the social behaviour of birds*. Frederick A. Praeger, Inc., Oxford, England.
- Tyler, C. W., Baseler, H. A., Kontsevich, L. L., Likova, L. T., Wade, A. R., and Wandell, B. A. (2005). Predominantly extra-retinotopic cortical response to pattern symmetry. *Neuroimage*, 24(2):306–314.
- van der Helm, P. A. and Leeuwenberg, E. L. J. (1996). Goodness of visual regularities: A nontransformational approach. *Psychological Review*, 103(3):429–456. Publisher: American Psychological Association.
- Wagemans, J., Van Gool, L., and d'Ydewalle, G. (1991). Detection of symmetry in tachistoscopically presented dot patterns: effects of multiple axes and skewing. *Perception & Psychophysics*, 50(5):413–27.
- Watson, A. B. and Pelli, D. G. (1983). Quest: A bayesian adaptive psychometric method. *Perception & Psychophysics*, 33(2):113–120.
- Webster, M. A. and MacLin, O. H. (1999). Figural aftereffects in the perception of faces. *Psychon Bull Rev*, 6(4):647–53.